HHS Public Access

Author manuscript

Stem Cell Res. Author manuscript; available in PMC 2021 January 05.

Published in final edited form as:

Stem Cell Res. 2020 December ; 49: 102078. doi:10.1016/j.scr.2020.102078.

Adaptation of the AID system for stem cell and transgenic mouse research

Marina V. Pryzhkova, **Michelle J. Xu**, **Philip W. Jordan***

Biochemistry and Molecular Biology Department, Johns Hopkins University Bloomberg School of Public Health, Baltimore, MD 21205, USA

Abstract

The auxin-inducible degron (AID) system is becoming a widely used method for rapid and reversible degradation of target proteins. This system has been successfully used to study gene and protein functions in eukaryotic cells and common model organisms, such as nematode and fruit fly. To date, applications of the AID system in mammalian stem cell research are limited. Furthermore, standard mouse models harboring the AID system have not been established. Here we have explored the utility of the *H11* safe-harbor locus for integration of the *TIR1* transgene, an essential component of auxin-based protein degradation system. We have shown that the *H11* locus can support constitutive and conditional *TIR1* expression in mouse and human embryonic stem cells, as well as in mice. We demonstrate that the AID system can be successfully employed for rapid degradation of stable proteins in embryonic stem cells, which is crucial for investigation of protein functions in quickly changing environments, such as stem cell proliferation and differentiation. As embryonic stem cells possess unlimited proliferative capacity, differentiation potential, and can mimic organ development, we believe that these research tools will be an applicable resource to a broad scientific audience.

Keywords

Auxin-inducible degron; Embryonic stem cells; SMC5/6 complex; *H11* locus; CRISPR-Cas9; Transgenic mouse

*Corresponding author. pjordan8@jhu.edu (P.W. Jordan).

CRediT authorship contribution statement

Marina V. Pryzhkova: Conceptualization, Methodology, Validation, Formal analysis, Investigation, Writing - original draft, Writing - review & editing, Visualization, Supervision, Project administration. **Michelle J. Xu:** Validation, Formal analysis, Investigation, Writing - original draft, Writing - review & editing, Visualization. **Philip W. Jordan:** Conceptualization, Methodology, Formal analysis, Investigation, Resources, Writing - original draft, Writing - review & editing, Visualization, Supervision, Project administration, Funding acquisition.

Author contributions

P.W.J and M.V.P conceived the project and designed experiments. M. V.P. established all cell lines. P.W.J. maintained transgenic mice. M.V.P. and M.J.X. performed all experiments. P.W.J, M.V.P. and M.J.X. analyzed the data and wrote the manuscript.

Declaration of Competing Interest

The authors declare that they have no known competing financial interests or personal relationships that could have appeared to influence the work reported in this paper.

Appendix A. Supplementary data

Supplementary data to this article can be found online at https://doi.org/10.1016/j.scr.2020.102078.

1. Introduction

Mouse and human embryonic stem cells (ESCs) are powerful tools for studying mammalian gene and protein function. The unlimited proliferative capacity and differentiation potential of ESCs allows for gain-and loss-of-function studies of numerous molecular processes and signaling pathways involved in stem cell maintenance, differentiation, and disease (Avior et al., 2016; Fisher et al., 2017; Gerlai, 2016; Lancaster and Huch, 2019; Li et al., 2018). Moreover, the ability of ESCs to contribute to embryonic development has facilitated the generation of transgenic mouse models and evaluation of protein function at the organism level (Gerlai, 2016; Tam and Rossant, 2003). Despite ESCs and mouse models being a versatile platform for the study of protein function *in vivo*, the current toolkit for achieving depletion of proteins of interest has limitations. Conventional RNA or gene targeting-based strategies to ablate protein function act at the pre-translational level. Gene knockout methods generally rely on the mutation or excision of a critical part of a gene, which results in irreversible protein loss or production of non-functional protein (Housden et al., 2017). Gene silencing at the RNA level involves blocking or destruction of target RNA sequences, which prevents translation of the corresponding protein. RNA targeting methods can be hindered by off-target effects and incomplete downregulation of protein expression (Housden et al., 2017). Time required for protein depletion using DNA or RNA level-acting approaches can span a few days and is dependent on mRNA stability and protein half-life. Extended protein depletion time can activate adaptive cellular response and prevent or hinder the evaluation of loss-of-function phenotype (El-Brolosy and Stainier, 2017; Housden et al., 2017). Thus, specific functions of highly stable proteins during dynamic phases of the cell cycle, stem cell differentiation, and stages of organism development cannot be accurately defined.

The development of systems for direct protein degradation have enabled studies of gene and protein functions in a simplified and prompt way. To date, several strategies utilizing conditional degrons or specific antibodies for controlling protein expression have been reported (Clift et al., 2017; Natsume and Kanemaki, 2017). The most widely used of these is the auxin-inducible degron (AID) technology. The AID system requires expression of *Oryza sativa* F-box transport inhibitor response 1 (TIR1) protein, which interacts with the native SCF E3 ubiquitin-ligase complex, and an AID-tagged target protein of interest (Nishimura et al., 2009). Addition of auxin mediates interaction between an AID-tagged protein and the TIR1-SCF E3 ubiquitin ligase complex, which leads to acute target protein degradation by the proteasome. Therefore, the AID system bypasses the aforementioned issues with traditional gene knockout and RNA interference (RNAi) systems. The AID system has been efficiently applied in vertebrate cells, yeast, nematodes and flies (Wood et al., 2016; Holland et al., 2012; Morawska and Ulrich, 2013; Perez-Arnaiz et al., 2016; Trost et al., 2016; Zhang et al., 2015; Bence et al., 2017). However, limited applications have been reported in ESCs (Baker et al., 2016; Brosh et al., 2016; Friman et al., 2019; Nora et al., 2017; Owens et al., 2019; Sybirna et al., 2020).

Functionality of the AID system depends on robust expression of the *TIR1* transgene (Nora et al., 2017). The site of *TIR1* integration is a very important factor to consider, particularly for ESCs, to ensure that *TIR1* is expressed and the AID system remains functional during differentiation. Approaches used to introduce the *TIR1* expression cassette in human somatic

cells have relied on random integration using viral vectors and, most recently, CRISPR-Cas9-mediated *AAVS1* safe harbor locus targeting (Holland et al., 2012; Natsume et al., 2016; Wutz et al., 2017). In human ESCs (hESCs), *TIR1* expression cassettes have been randomly integrated using lentiviral and PiggyBac transposon vectors (Brosh et al., 2016; Sybirna et al., 2020). However, random integration of a transgene limits control of protein production, is prone to transgene silencing, and can introduce variability in the obtained results (Irion et al., 2007; Nora et al., 2017; Smith et al., 2008). Moreover, disruption of the genome by random integration events can have significant consequences that are not always readily apparent (Sakurai et al., 2010; Staal et al., 2008). In mouse ESCs (mESCs) *TIR1* has been integrated at *TIGRE* and *Rosa26* loci (Nora et al., 2017; Baker et al., 2016). A potential drawback of *TIGRE* and *Rosa26* loci is that they are located within endogenous genes and can display differential transgene expression depending on the promoter and specific cell type (Casola, 2010; Nora et al., 2017; Zeng et al., 2008).

To extend applications of the AID system in stem cell and animal research, we have evaluated the *Hipp11* (*H11*) safe harbor locus as a potential site for integration of the *TIR1* expression cassette (Hippenmeyer et al., 2010; Tasic et al., 2011; Zhu et al., 2014). The *H11* locus is located in a transcriptionally active intergenic region and is advantageous over the more widely used *Rosa26* locus due to higher rate of recombination, targeting efficiency, and level of transgene expression *in vivo* in mice (Hippenmeyer et al., 2010; Tasic et al., 2011; Chen-Tsai, 2020). Similarly, transgene targeting into the human *H11* locus is efficient and permits stable transgene expression in hESCs and their differentiated derivatives, which makes this locus preferential compared to commonly used *AAVS1, ROSA26,* and *HPRT1* loci (Smith et al., 2008; Di Domenico et al., 2008; Irion et al., 2007; Zhu et al., 2014).

To assess the functionality of the AID system with *H11* locus-integrated *TIR1*, we AID-tagged core components of the structural maintenance of chromosomes complex, SMC5/6. The SMC5/6 complex is required for maintaining genome stability through its involvement in DNA replication, homologous recombination, and chromosome segregation (Aragón, 2018). Our previous studies utilizing the Cre recombinase-mediated conditional knockout (cKO) approach have shown that core proteins of the SMC5/6 complex are highly stable and require at least two days to achieve protein depletion (Hwang et al., 2017; Pryzhkova and Jordan, 2016).

In this study, we present successful integration of the AID system into mouse and human ESCs and detail the production of transgenic mice that express *TIR1* in a constitutive and Cre-inducible manner. We show that the *H11* locus can be utilized for *TIR1* expression and demonstrate that the AID system is effective for degradation of stable, long-lived proteins. These research tools will be a valuable resource to a broad scientific research audience.

2. Materials and methods

2.1. Mouse use and care

All mice were bred at Johns Hopkins University (JHU, Baltimore, MD) in accordance with the National Institutes of Health and U.S. Department of Agriculture criteria and protocols for their care and use were approved by the Institutional Animal Care and Use Committees

(IACUC) of JHU. The following mouse strains were used: C57BL/6J (B6/J), stock number 000664 (Jackson Laboratory (JAX)); 129S1/SvImJ (129S1), stock number 002448 (JAX); B6.Cg-*Edil3*$^{Tg(Sox2\text{-}cre)1Amc}$/J (*Sox2-Cre*), stock number 008454 (JAX); B6.129S2-*Emx1*$^{tm1(cre)Krj}$/J (*Emx1-Cre*), stock number 005628 (JAX); *Spo11-Cre* (Lyndaker et al., 2013), B6(Cg)-*Tyrc-2J*/J (B6 albino), stock number 000058 (JAX); Hsd: ICR (CD-1) (Envigo).

2.2. Transgenic mice generation

Chimeric mice were generated using methods previously described (Nagy et al., 2003). Briefly, blastocyst stage embryos were obtained from superovulated females mated to same strain males. Targeted embryonic stem cells were injected into the blastocyst of each embryo (~12–15 per embryo). Following injection, surviving embryos were surgically transferred to oviducts of pseudo-pregnant CD-1 females (Envigo) (~15 embryos/female). B6 mESCs were injected into B6 albino blastocysts. 129 mESCs were injected into B6/J blastocysts. Chimeras were further bred to females of the same genetic background as that of the ES cells. Obtained transgenic animals were further bred to establish colonies.

2.3. mESCs

B6 mESCs used in this study were established and maintained in 2i/LIF medium as previously described (Pryzhkova and Jordan, 2016). 129S6/SvEvTac (129S6) mESCs (Taconic Biosciences) were obtained from JHU Transgenic Mouse Core. mESCs from TIR1 transgenic animals were established and maintained in 2i/LIF medium as described in (Pryzhkova and Jordan, 2016) with exception that mESCs were established from pooled embryos. Briefly, mESC culture medium included 1:1 mixture of DMEM/F12 (Gibco) and Neurobasal medium (Gibco) with 1% N2 supplement (Gibco) and 2% B27 supplement (Gibco), 1 mM L-Glutamine (Gibco), 1% MEM NEAA (Gibco), 50 μM β-mercaptoethanol (Gibco), 50 μg/ml BSA (Sigma), 10 ng/ml human LIF (PeproTech), 1 μM MEK inhibitor PD 0325901 (Cayman) and 3 μM GSK-3 inhibitor CHIR 99021 (Cayman). Cells were grown under feeder-free conditions on 0.2% gelatin (Sigma) and passaged every 3 days with TrypLE Express (Gibco). Essential reagent information is provided in Table S3.

2.4. Neural differentiation

A day before passaging mESCs were switched to a neural differentiation medium consisting of 2i medium without human LIF, MEKi and GSK-3i, and supplemented with 10 ng/ml human bFGF (PeproTech). Cells were passaged as small clumps onto uncoated cell culture vessels. One third of medium was replaced with fresh medium every other day. Cells were grown in suspension with gentle mechanical dissociation at the time of medium change. In a parallel experiment, 5% FBS (HyClone) was added to neural differentiation medium.

2.5. hESCs

hESC line H1 (WiCell, Madison, WI, USA) was used in this study. The use of the hESC line was approved by JHU institutional stem cell research oversight committee (protocol ISCRO00000089). hESCs were maintained in Essential 8 medium (Gibco) on Geltrex (Gibco)-coated tissue culture plates as previously described (Pryzhkova and Jordan, 2020).

Cells were routinely passaged every 5 days with 0.5 mM EDTA in PBS with a split ratio of 1:6–1:10. Key reagent information is provided in Table S3.

2.6. Primary cultures

Primary cell cultures were maintained in DMEM/F12 (Gibco) supplemented with 10% FBS (HyClone) and penicillin-streptomycin (100 U/100 μg, Gibco). Mouse lung tissue was minced with scissors and placed in culture medium onto cell culture vessels. Tail tips were first embedded into Geltrex (Gibco) to allow for cell outgrowth. Cells were passaged with 0.05% trypsin–EDTA (Gibco). Following expansion cells were collected for analysis.

2.7. ESC transfection and chemical treatment

Plasmids were delivered into mouse and human ESCs using LipoJet (SignaGen). Transfection was performed following manufacturer protocol in 6-well plates overnight, unless specified differently. In total, 2 μg of DNAs were added into one well. Two plasmids were used for gene targeting: one carrying Cas9 nuclease and gRNA(s), and a second carrying donor DNA for site-specific recombination. A ratio 1:2 was used for Cas9-gRNA vector and donor DNA vector. Selection was initiated 24 h after removal of transfection reagents for mESCs and 48 h for hESCs.

mESCs were selected with 80 μg/ml hygromycin (Sigma) or 1 μg/ml puromycin (Sigma) for the first 2–3 days, then the dose was decreased to 50 μg/ml hygromycin or 0.5 μg/ml puromycin. Cells were grown in the presence of selective drugs until single cell-derived clones were expanded and stocks were frozen.

hESCs were selected with 0.25 μg/ml puromycin until single colonies have appeared. Then individual colonies were picked and expanded. After establishing, hESC lines were continuously grown in the presence of 0.5 μg/ml puromycin. For *SMC6* targeting hESC transfection was performed for 48 h and in the presence of 5 μM ROCKi (Hello Bio). Selection with 100 μg/ml G418 (Corning) was started 24 h after removal of transfection reagent and in the presence of ROCKi for first 2–3 days. Then cells were continuously grown in the presence of 50 μg/ml G418.

Puromycin and G418 were withdrawn from cell culture medium a day before passaging and on the day of passaging. Drugs can be safely added back to the medium once cells have attached. To establish homozygous and heterozygous hESC lines, cells were plated at low density as small clumps or as single cells (in the presence of 5 μM ROCKi). Established colonies were genotyped and expanded.

In all experiments, mouse and human ESCs were treated with 100 μM indole-3-acetic acid (IAA, Sigma) for the time specified, except 500 μM IAA was used for SMC6 protein depletion in hESCs.

2.8. DNA construct design

The design of Cas9-gRNA vector including eSpCas9(1.1) and two gRNAs is described in (Pryzhkova and Jordan, 2020). This vector was used to target mouse and human *H11* loci and mouse *Smc5* gene. pX330 (Addgene, #42230) including SpCas9 and one gRNA was

used for human *SMC6* targeting. gRNAs were selected using Zhang Lab software (Hsu et al., 2013). gRNA sequences are provided in Table S1.

Donor vector design for human *H11* locus targeting is described in (Pryzhkova and Jordan, 2020), except instead of fluorescent protein coding sequence there is HA-tagged *TIR1* sequence (pRAIDRS, kind gift from Dr. Brosh). The vector utilized for human *H11* locus targeting also was used for mouse *H11* locus targeting with modifications: homology arms were amplified from B6 mouse genomic DNA so that 5′ homology arm (689 bp) spans 3 bp away from the cut site and 3′ homology arm (720 bp) spans 5 bp away from the cut site. To make *TIR1* vector for conditional expression, this vector was cut at SgrDI restriction site between EF1α promoter and *TIR1* sequence, and PCR-amplified floxed STOP cassette (Addgene, #85006) was incorporated using In Fusion HD cloning kit (Clontech).

Donor vector for mouse *Smc5* targeting includes a part of intron and the last *Smc5* exon amplified from B6 mouse genomic DNA, followed by DDK-tagged mini-AID (AID47) (pRAIDRS, kind gift from Dr. Brosh). Donor vector also includes hygromycin resistance gene driven by mouse PGK promoter and flanked by *LoxP* sites (Addgene, #51423). Homology arms were amplified from B6 mouse genomic DNA. The 5′ homology arm (971 bp) and 3′ homology arm (1019 bp) span 5 bp away from the cut sites. To prevent recutting of donor DNA with Cas9 nuclease, the first nucleotide in 5′ homology arm was replaced so that PAM sequence became “NGC”.

Donor vector for human *SMC6* targeting includes DDK-tagged mini-AID (AID46) (Addgene, #101713) (Lambrus et al., 2018), followed by floxed neomycin resistance gene driven by human PGK promoter. The 5′ homology arm (328 bp) restores the cut site in the last exon of *SMC6* gene, and 3′ homology arm (330 bp) starts 1 bp away from cut site, immediately from STOP codon.

To facilitate conditional TIR1 expression in cell culture we used pCAG-Cre:GFP (Addgene, #13776).

GenBank (Snapgene) files containing plasmid maps and sequences are provided as Supplementary information.

2.9. Genotyping

DNA was extracted using the GeneJet Genomic DNA purification kit (Thermo Scientific) and 25 ng was used for each PCR. Alternatively, cells were lysed with Lairds buffer (100 mM Tris pH 8.5, 5 mM EDTA, 0.2% SDS, 200 mM NaCl) and proteinase K. DNA was precipitated with isopropanol. The pellet was resuspended in molecular grade water (Sigma), and 25 ng DNA were used for each PCR. PCR reactions were set with AccuStart II PCR SuperMix (Quanta BioSciences) (Pryzhkova and Jordan, 2020). Primers and PCR conditions are listed in Table S4.

2.10. Semi-quantitative RT-PCR

Total RNA was isolated using PureLink RNA kit (Ambion) followed by DNase I (RNase-free, Ambion) treatment. First strand cDNA synthesis was carried out using M-MuLV

reverse transcriptase and random primer mix (NEB) under following conditions: 25 °C for 5 min, 42 °C for 1 h, 65 °C for 20 min. PCR amplification of cDNA samples was set with AccuStart II PCR SuperMix (Quanta BioSciences) (Pryzhkova and Jordan, 2020). Primers and PCR conditions are listed in Table S5.

2.11. Western blot analysis

Cell lysates were prepared in RIPA buffer (Santa Cruz Biotechnology) supplemented with protease inhibitor cocktail (Roche). Equal amounts of proteins were fractionated by SDS-PAGE and transferred to PVDF membrane (Bio-Rad). For protein analysis, 6.5% gels were used for SMC5 and SMC6 and 7.5% gels were used for TIR1. For some gels 0.5% 2,2,2-trichloroethanol (TCE) was added into resolving gel to visualize protein load for each sample. Antibodies used are provided in Supplementary Table S6. All blocking and incubation with antibodies was performed in Western Blocker Solution (Sigma). Signal was detected using Clarity Western ECL Substrate (Bio-Rad) and imaged using Syngene XR5 system. SMC5 protein depletion in mESCs was analyzed using GeneTools software (Syngene).

2.12. Immunocytochemistry

Single mESCs were fixed in suspension in 10% formalin (Sigma) for 15 min at room temperature, washed in PBS (Life Technologies) and ~50,000 cells were spun onto glass slides using Shandon Cytospin 4 centrifuge (Thermo Fisher Scientific). Immunocytochemistry was performed as previously descried (Pryzhkova and Jordan, 2020). Cells were mounted with Vectashield Mounting Medium with DAPI (Vector Laboratories). Antibodies used are provided in Table S6.

2.13. Microscopy

Immunofluorescence analysis and image capture were performed using either a Zeiss Axio Imager.A2 and AxioCam MRm (Zeiss), Zeiss CellObserver Z1 microscope linked to an ORCA-Flash 4.0 CMOS camera (Hamamatsu), or Keyence BZ-800 and BZ-X800 Viewer and Analyzer software. Images were processed using ZEN 2012 blue edition imaging software (Zeiss) or BZ-X800 Viewer and Analyzer software (Keyence). Photoshop (Adobe) was used to prepare figure images (Hwang et al., 2017; Pryzhkova and Jordan, 2020).

2.14. Statistical analysis

Statistical tests were performed with RStudio and GraphPad Prism 8. For mESC mitotic analyses, statistical significance was assessed by Pearson's chi-squared test. Yates' continuity correction was applied, since data were binomially distributed and discrete with sample size less than 100. Percentage of normal anaphases in untreated and IAA-treated groups were compared. At least 50 cells were analyzed per cell line for each experimental condition. The weighted mean with weighted standard deviation of three experiments is shown on graphs. For mESC growth analysis, statistical significance was assessed by unpaired Student's *t* test (two-tailed) using the mean and standard deviation of four experiments. For all analyses, a value of $p < 0.05$ was considered significant.

3. Results

3.1. Integration of TIR1 expression cassette into H11 locus in mESCs

In this study, we used CRISPR-Cas9 genome editing to incorporate a *TIR1* expression cassette into the *H11* locus in C57BL/6J (B6) and 129S6/SvEvTac (129) mESC lines (Hippenmeyer et al., 2010; Tasic et al., 2011; Chen-Tsai, 2020). We employed the *Streptococcus pyogenes* Cas9 (eSpCas9(1.1)) nuclease, which has been optimized to reduce chances of off-target mutations (Slaymaker et al., 2016). In addition, we adopted a dual-guide RNA (gRNA) targeting approach, which introduces two double-strand breaks in genomic DNA and has been reported to increase homologous recombination and gene targeting efficiency in ESCs (Chen et al., 2015; Oji et al., 2016). A pair of gRNAs were chosen to introduce genomic deletion of 1175 bp in the *H11* locus (Fig. 1a, Table S1).

The donor vector included codon-optimized sequence for *Oryza sativa* TIR1 auxin receptor (TIR1) driven by the elongation factor 1α (EF1α) promoter (Fig. 1a) (Brosh et al., 2016). To be able to evaluate TIR1 expression directly, we added human influenza hemagglutinin (HA) tag at the C-terminus. The donor construct harbored a puromycin N-acetyltransferase (Puro) cassette conferring puromycin resistance driven by mouse phosphoglycerate kinase-1 (PGK) promoter (Fig. 1a). Tissue-specific transgene expression is often required when using ESCs for differentiation studies or to create transgenic animals. Thus, we generated two versions of donor construct for *TIR1* expression. One construct (V1-TIR1) was designed for constitutive expression of *TIR1* and has Puro selection cassette flanked by *LoxP* sites (Fig. 1a). This construct was introduced into B6 and 129 mESCs. The second construct (V2-TIR1) includes a STOP cassette flanked by *LoxP* sites that is positioned between *EF1α* promoter and *TIR1* transgene. The Puro selection cassette within the V2-TIR1 construct is flanked by *FRT* sites (Fig. 1a). This construct allows for conditional Cre recombinase-mediated *TIR1* expression. This DNA construct was integrated into *H11* locus of 129 mESCs.

After puromycin selection, we genotyped B6 mESCs with V1-*TIR1* ($B6^{V1\text{-}TIR1}$) (Fig. 1b, Fig. S1a, b) and identified 39% heterozygous and 28% homozygous clones (Table S2, Fig. S1b). Other clones contained one targeted allele and one allele harboring a deletion and were excluded from further studies (Table S2, Fig. S1b). Immunoblotting for TIR1 expression using anti-HA tag antibodies allowed for efficient detection of protein expression (Fig. 1c).

For 129 mESCs with constitutive V1-*TIR1* ($129^{V1\text{-}TIR1}$) we obtained 23% homozygous and 23% heterozygous clones (Table S2, Fig. S1c). In 129 mESCs with conditional V2-*TIR1* ($129^{V2\text{-}TIR1}$) we identified 17% homozygous and 28% heterozygous clones (Table S2, Fig. S1d). The decreased targeting efficiency with V2-*TIR1* probably reflects the increase in the size of the donor DNA construct due to incorporation of STOP cassette (~1.4 kb). We further evaluated $129^{V2\text{-}TIR1}$ mESCs at different time points after transient *Cre* recombinase transfection (Fig. 1d, e, Fig. S2a–c). The efficient STOP cassette excision and TIR1 protein expression were readily detected by twelve hours post- transfection (Fig. 1d, e). All analyzed clones demonstrated TIR1 expression after Cre-mediated STOP cassette removal (Fig. 1d, e, Fig. S2a–c).

It has been reported that transgene expression can variegate upon ESC differentiation (Nora et al., 2017). To ensure stable TIR1 protein levels in differentiated cells, we cultured $B6^{V1\text{-}TIR1}$ mESCs under neural differentiation conditions and verified the presence of the protein after twenty days of culture (Fig. S2d, e). Furthermore, the addition of auxin did not affect TIR1 levels, although levels of protein were decreased in differentiated cells (Fig. S2d, e).

Thus, we have shown that the *H11* locus can be efficiently targeted using CRISPR-Cas9 technology and successfully used for constitutive and Cre-inducible TIR1 expression in B6 and 129 mESCs.

3.2. Evaluation of TIR1 expression in mice

Transgenic mouse models are a versatile tool for studying gene and protein functions, investigating mammalian development, and disease modeling (Ericsson et al., 2013). Mice with integrated AID system would allow for precise control of protein expression *in vivo*. To generate *TIR1* transgenic mice, we utilized $B6^{V1\text{-}TIR1}$ mESCs constitutively expressing *TIR1* and $129^{V2\text{-}TIR1}$ mESCs with conditional *TIR1* expression. The $B6^{V1\text{-}TIR1}$ and $129^{V2\text{-}TIR1}$ mESCs successfully contributed to chimera formation and underwent germline transmission (Fig. 2, Fig. S3a).

To ensure that an active and functional *TIR1* transgene was stably inherited by the next generations, the progeny of mouse founders from both strains were evaluated for *TIR1* transgene expression at the RNA and protein level (Fig. 2a, b, Fig. S3b). mESCs established from blastocysts of $B6^{V1\text{-}TIR1}$ transgenic mice demonstrated protein expression level similar to that of the original transgenic mESCs (Fig. 2b). We also established mESCs from embryos of $129^{V2\text{-}TIR1}$ mice. These cells were transiently transfected with the *Cre* recombinase construct to remove the floxed STOP cassette and allow for transgene expression (Fig. S2a). As with the parental $129^{V2\text{-}TIR1}$ mESCs, *Cre* transfection led to upregulation of TIR1 protein expression in rederived mESCs (Fig. 2b). Additionally, we evaluated the efficiency of STOP cassette removal *in vivo*. For this experiment, $129^{V2\text{-}TIR1}$ transgenic mice were bred with mice carrying the germ cell-specific *Spo11-Cre* transgene to generate animals constitutively expressing *TIR1*, which were used to obtain blastocysts and derive mESCs (Fig. 2a). As shown in Fig. 2b, TIR1 protein was readily detected in mESCs following Cre excision mediated *in vivo*.

We next assessed the presence of *TIR1* RNA in different tissues of $B6^{V1\text{-}TIR1}$ mice, such as lungs, tail tip fibroblasts, and cortex (Fig. 2c). *TIR1* RNA was readily detected in all 20 transgenic mice analyzed. We also bred $B6^{V1\text{-}TIR1}$ mice with mice carrying *Sox2-Cre* and assessed *TIR1* expression after excision of the puromycin selection cassette, confirmed by genotyping (Fig. S3c, d). Our results show that the selection cassette can be removed *in vivo* using Cre recombinase without affecting *TIR1* expression (Fig. 2c).

To evaluate Cre-inducible *TIR1* expression, we bred $129^{V2\text{-}TIR1}$ mice with *Emx1-Cre* mice (Fig. 2a). Embryonic cortices at 12.5 days post coitum (dpc) were analyzed for STOP cassette excision and transgene expression (Fig. 2d, e, Fig. S2a). Our results demonstrate

that Cre-mediated STOP cassette removal allowed for *TIR1* transgene expression in 129 $^{V2\text{-}TIR1}$ mice *in vivo*.

Thus, our study shows that TIR1-expressing mESCs established from B6 and 129 mouse strains contribute to the germline and allow for the transmission of a functional transgene to the progeny. Further generation and evaluation of transgenic mice carrying both *TIR1* and *AID*-tagged genes of interest will demonstrate the functionality of the AID system *in vivo*.

3.3. Smc5 locus targeting and evaluation of auxin-mediated protein degradation

The structural maintenance of chromosomes complex, SMC5/6, plays a crucial role in DNA replication, DNA damage repair, and chromosome segregation (Aragón, 2018). We have previously shown that SMC5/6 complex is indispensable for ESC genome integrity (Pryzhkova and Jordan, 2016). In that study, we used mESCs harboring a *Smc5* conditional knockout allele mutated using tamoxifen-inducible Cre recombinase. However, the conditional knockout system required up to two days for protein depletion in cell culture. In contrast, the AID system offers fast and reversible protein degradation, thus, permitting the evaluation of immediate effects of protein loss on cellular processes (Baker et al., 2016; Brosh et al., 2016; Natsume et al., 2016; Nora et al., 2017).

To validate the AID system functionality in our mESC lines we employed a similar targeting strategy as described for the *H11* locus. Two gRNAs were selected to make double-stranded DNA breaks in the last intron of *Smc5* and adjacent 3′ UTR region (Fig. 3a, Table S1). After homology-directed repair the removed fragment is replaced by the last *Smc5* exon tagged with *AID* and *DDK*, followed by a floxed hygromycin resistance cassette (Fig. 3a). In our study we used a human codon- optimized minimal required AID degron (AID47) (Brosh et al., 2016).

One homozygous and one heterozygous B6$^{V1\text{-}TIR1}$ mESC lines and one heterozygous 129 $^{V2\text{-}TIR1}$ mESC line were used for *Smc5* locus targeting. After hygromycin selection, obtained clones were genotyped as shown in Fig. 3b and Fig. S4a. The *Smc5* locus targeting resulted in 35% (8 clones) *Smc5-AID* heterozygous and 22% (5 clones) *Smc5-AID* homozygous B6$^{V1\text{-}TIR1}$ mESC clones. Due to efficient targeting, only a few 129 $^{V2\text{-}TIR1}$ mESC clones were screened. Two clones, *Smc5-AID* heterozygous and homozygous, were analyzed for each parental *TIR1* transgenic mESC line (Fig. 3c–h).

After addition of auxin to targeted B6$^{V1\text{-}TIR1}$ mESCs we observed robust depletion of SMC5 after one hour of treatment (Fig. 3d, f, Fig. S4b, c, Fig. S5a, b). SMC5 depletion was detected using antibodies against SMC5 protein and DDK tag in both *Smc5-AID* homozygous and heterozygous cell lines (Fig. 3d, f, Fig. S4b, c). Expression of TIR1 from one or two alleles did not affect the efficiency of SMC5 protein depletion (Fig. 3d, f, Fig. S4b, c, Fig. S5a, b). Similar results were obtained in 129 $^{V2\text{-}TIR1}$ cell lines (Fig. 3g,h, Fig. S4d, e, Fig. S5c). After 24 h of transient *Cre* transfection cells were treated with auxin. Efficient SMC5 depletion was observed after one hour of treatment (Fig. 3h, Fig. S4d, e, Fig. S5c).

Our results demonstrate functionality of the AID system in mESCs, when TIR1 protein is expressed constitutively or conditionally from the *H11* locus. Furthermore, we show that the AID system is superior over conventional approaches for perturbing gene functions and allows for rapid degradation of stable proteins.

3.4. AID system allows for rapid evaluation of SMC5 depletion phenotype

In a previous study, we showed that conditional mutation of *Smc5* in mESCs using tamoxifen-inducible recombinase results in chromosome missegregation, mitotic catastrophe and cell death, observable four to five days after the initiation of tamoxifen treatment (Pryzhkova and Jordan, 2016). In contrast, significant decrease in cell number was readily detected two days after auxin treatment (Fig. 4a). *Smc5-AID* homozygous $B6^{V1\text{-}TIR1}$ mESCs treated for two and five days with auxin showed decline in cell numbers by 2.4- and 14-fold, respectively, compared to untreated control (Fig. 4a). Cell growth was not significantly affected in auxin-treated *Smc5-AID* heterozygous cells (Fig. 4a). Complementing our previous findings, we observed an increase in chromosome missegregation, lagging chromosomes and DNA bridges during mitosis (Fig. 4b, c). More specifically, 66% of abnormal mitotic cells were observed as early as 12 h after auxin treatment. The percentage of cells with mitotic abnormalities increased to 85% after 48 h, in striking contrast to an average of 28% for control cells (Fig. 4b).

These results confirm the crucial role of the SMC5/6 complex in maintenance of genome integrity in pluripotent stem cells, as well as underline the superiority of the AID system over conventional techniques used to evaluate protein functions.

3.5. Incorporation of AID system into hESCs

Introducing the AID system into hESCs provides the opportunity to investigate functions of diverse proteins not only in stem cells, but also their differentiated derivatives, in a physiologically-relevant and human species-specific manner (Avior et al., 2016; Gabdoulline et al., 2015). So far, the use of the AID system in hESCs has been limited, and further improvement is needed to extend its applications in human stem cell research (Brosh et al., 2016; Sybirna et al., 2020). Previous work has relied on random integration of *TIR1* expression cassette using a lentiviral vector or the PiggyBac transposon system (Brosh et al., 2016; Sybirna et al., 2020). However, random integration of a transgene introduces uncertainty and variability and can have undesired consequences (Irion et al., 2007; Sakurai et al., 2010; Smith et al., 2008; Staal et al., 2008). Therefore, we sought to incorporate constitutive *TIR1* transgene into the human *H11* locus, which has been reported as a safe, transcriptionally active locus providing robust expression of inserted transgenes in hESCs (Zhu et al., 2014). We have previously shown that the *H11* locus can be targeted using CRISPR-Cas9 approach and allows for stable constitutive expression of fluorescent proteins in hESCs (Pryzhkova and Jordan, 2020). Therefore, we incorporated a *TIR1* expression cassette into the *H11* locus using the same strategy as described for mESCs (Fig. 5a). After selection with puromycin, we genotyped drug-resistant clones to confirm transgene integration (Fig. 5b, Fig. S6a, b). Five from eight successfully targeted heterozygous clones demonstrated sustained TIR1 expression (Fig. 5c).

To validate the functionality of the AID system, we tagged *SMC6* in hESCs stably expressing TIR1. We used a single gRNA to make a DNA double-strand break near the stop codon. The donor construct contained the codon-optimized minimal-required AID degron (AID46) followed by a *DDK* tag and floxed neomycin resistance cassette (Fig. 5d) (Lambrus et al., 2018). Successful *SMC6* targeting was confirmed by genotyping and protein expression analysis (Fig. 5e, f, Fig. S6c, d). Similar to the phenotype observed with mESCs, SMC6 depletion dramatically affected hESC proliferation (Fig. S7a). Auxin treatment of parental TIR1-expressing hESC line did not cause negative effects on cell growth (Fig. S7b).

Next, we performed subcloning of the mixed population of cells and established heterozygous (15 clones) and homozygous (13 clones) *SMC6-AID* cell lines. Cell lines were genotyped, and AID-tagged version of SMC6 was confirmed by western blot (Fig. 5g, h, Fig. S6e). SMC6 depletion was observable after 2–3 h of auxin treatment and appeared to be less efficient compared to one hour in mouse ESCs (Fig. 5i, Fig. S6f, Fig. 3d, f, h).

Thus, we have shown that the human *H11* locus can be successfully utilized for integration of *TIR1* transgene. Furthermore, we have demonstrated that the AID system can be employed for studying SMC5/ 6 complex functions in hESCs.

4. Discussion

The AID system ensures specific, fast, titratable, and reversible degradation of a target protein and affords the opportunity to investigate complex biological processes in a fine-tuned manner in mammalian ESCs (Fig. 6). Limited studies have employed the AID system to investigate ESC genomic organization, DNA damage response, factors required to maintain stem cell pluripotency, as well as human germ cell specification (Brosh et al., 2016; Friman et al., 2019; Nora et al., 2017; Sybirna et al., 2020). Early reports utilizing the AID system in somatic, cancer and ES cells relied on expression of an AID-tagged transgene and the suppression of endogenous gene function by RNAi, which greatly limited applications of the AID system (Brosh et al., 2016; Holland et al., 2012; Nishimura et al., 2009). The development of CRISPR-Cas9 genome-editing technology has streamlined the process of endogenous gene tagging in mESCs (Baker et al., 2016; Natsume et al., 2016). However, optimal integration site for *TIR1* expression cassette still needs further improvement. The sustained expression of auxin-interacting F-box protein TIR1 is a requisite for efficient AID-tagged protein degradation by the proteasome (Nora et al., 2017). Initial experiments in human somatic cells employed random, virus-mediated *TIR1* transgene integration (Holland et al., 2012; Lambrus et al., 2015). Later, the *AAVS1* safe harbor locus was evaluated and used for defined TIR1 expression (Li et al., 2019; Natsume et al., 2016; Sathyan et al., 2019). However, prior to our work, only random lentivirus and transposon- based incorporation of *TIR1* expression cassette was utilized in hESCs (Brosh et al., 2016; Sybirna et al., 2020). These approaches can result in the disruption of endogenous genes, multiple integration sites and variegation of transgene expression, potentially resulting in obscured phenotypes (Irion et al., 2007; Nora et al., 2017; Sakurai et al., 2010; Smith et al., 2008; Staal et al., 2008). In mESCs, *TIR1* transgene was integrated into commonly used *Rosa26* and *TIGRE* loci using CRISPR- Cas9 (Baker et al., 2016; Nora et al., 2017). Although, *TIGRE* was reported to be preferential for TIR1 expression in mESCs

over *Rosa26*, both loci are positioned in endogenous genes and transgene expression is affected by the local transcriptional activity (Casola, 2010; Strathdee et al., 2006; Zeng et al., 2008).

In our study we used CRISPR-Cas9 technique and chose dual gRNA approach to incorporate *TIR1* expression cassette into human and mouse safe-harbor locus *H11* (Chen et al., 2015; Oji et al., 2016). The *H11* locus has been reported to be superior to other commonly used loci in mouse and human genomes due to intergenic location, stable transgene expression, and higher targeting efficiency (Hippenmeyer et al., 2010; Tasic et al., 2011; Zhu et al., 2014). We have successfully generated homozygous and heterozygous *TIR1* transgenic mESC lines and demonstrated stable protein expression in cell lines with constitutive and conditional *TIR1* expression. A previous study utilizing random *TIR1* integration in mESCs has mentioned downregulation of TIR1 protein levels upon differentiation into neural lineage (Nora et al., 2017). We confirmed the persistence of TIR1 after continuous mESC culture under neural differentiation conditions, albeit at lower levels (Fig. S2d, e).

To evaluate the AID system functionality, we AID-tagged core proteins of SMC5/6 complex in mouse and human ESCs. Our previous studies have shown that SMC5 and SMC6 proteins are very stable and require extended time to undergo degradation (Hwang et al., 2017; Pryzhkova and Jordan, 2016; Gaddipati et al., 2019). Attempts to study SMC5/6 functions in human somatic cells using RNAi approach appeared complicated due to off-target effects and induction of non- related phenotypes (Wu et al., 2012). Moreover, the phenotype observed after SMC5/6 protein depletion using approaches acting at DNA and RNA level seems to be species- and cell type-dependent (Fazzio and Panning, 2010; Gallego-Paez et al., 2014; Nishide and Hirano, 2014; Stephan et al., 2011). Initially, we employed a tamoxifen-inducible conditional knockout strategy to investigate the role of SMC5/6 complex in mESCs and embryonic fibroblasts. While efficient genomic DNA excision and protein depletion requires two days in mESCs, up to five days is needed for mouse fibroblasts (Gaddipati et al., 2019; Pryzhkova and Jordan, 2016). Here, we have demonstrated that the AID system outperforms traditional approaches employed for SMC5/6 complex studies. The AID system allows for degradation of highly stable proteins within only one hour of auxin addition and detection of a distinct phenotype, such as inability to segregate chromosomes properly, as early as twelve hours after auxin addition (Fig. 4b, c). Moreover, we have demonstrated the applicability of the AID system for SMC6 protein depletion in hESCs (Fig. 5i, Fig. S6f). Previous studies have shown that ubiquitous expression of TIR1 can cause auxin-independent “basal degradation” of some proteins of interest, leading to the recent development of systems with improved control (Li et al., 2019; Natsume et al., 2016; Sathyan et al., 2019; Yesbolatova et al., 2019). However, we did not observe a significant effect of this phenomenon in our study, likely due to the stability and high expression of SMC5 and SMC6 proteins.

While ESCs have enormous potential for reconstructing biological processes in cell culture *in vitro*, mice continue to be the most widely used system for *in vivo* research (Ericsson et al., 2013; Gerlai, 2016). Current studies utilizing the AID system are limited to research on mouse oocytes and early developmental stage embryos, and evaluation of phenotype by

means of fluorescence microscopy (Borsos et al., 2019; Camlin and Evans, 2019; Gu et al., 2018; Miura et al., 2018). The generation of mouse models with an integrated AID system provides the opportunity to study protein functions in a timely manner at an organism level (Fig. 6). Ubiquitous expression of TIR1 would allow for the simultaneous depletion of a protein of interest in the whole organism, whereas conditional Cre-mediated TIR1 expression would be more suitable for loss-of-function experiments in specific tissues. Numerous mouse strains carrying *Cre* transgene regulated by tissue-specific promoters have been developed (Kim et al., 2018). This widely extends applications of mouse models with an integrated AID system. In our study, we have generated transgenic mouse strains with either constitutive or conditional *TIR1* expression. We have shown that constitutive transgene expression is readily detected at RNA level in different tissues of mice, and *TIR1* expression can be activated *in vivo* using tissue-specific Cre recombinases. Furthermore, we have demonstrated stable transmission of the functional transgene to progeny.

Further studies are needed to assess TIR1 expression in mouse tissues at the protein level and to assess the functionality of the AID system *in vivo*. Generation of mice with an integrated AID system requires AID-tagging of the gene of interest. The development of CRISPR-Cas9 technology has made mouse genome targeting in zygotes more simple and efficient compared to traditional approaches, including pronuclear microinjection of recombinant DNA or blastocyst injection with mESCs preselected for the desired transgene (Chen et al., 2016; Qin et al., 2015; Tröder et al., 2018; Wang et al., 2016). CRISPR-Cas9 technology currently allows tagging of endogenous mouse genes precisely and with high efficiency using PCR-amplified DNA oligonucleotides up to 1 kb long with only ~ 35 bp homology arms (Paix et al., 2017). The length of commonly used truncated AID tags ranges from 132 bp to 204 bp (Brosh et al., 2016; Lambrus et al., 2018; Morawska and Ulrich, 2013; Natsume et al., 2016). Thus, AID tagging endogenous genes of interest in mouse zygotes obtained from TIR1-expressing mice shows promise to be feasible and efficient (Fig. 6).

Auxin is inexpensive, widely available and can be administered to mice at doses exceeding 50 mg/kg per day without adverse effects during fetal or post-natal development (John et al., 1979; Mourão et al., 2009). Since the AID system has not been tested in mice, further adjustments of auxin doses will be required to obtain satisfactory protein depletion. Alternatively, the AID system can be utilized in *ex vivo* organotypic culture, often required in mouse research (Croft et al., 2019; Sato et al., 2015; Shamir and Ewald, 2014).

In closing, we have evaluated the *H11* locus for ubiquitous and conditional *TIR1* expression in mouse and human ESCs, as well as in mice. We have demonstrated the superiority of the AID system over traditional approaches for loss-of function studies of stable proteins. We believe that the research tools we have developed can help advance stem cell research and be extended to *in vivo* experiments in mice.

Supplementary Material

Refer to Web version on PubMed Central for supplementary material.

Acknowledgements

We thank JHU Transgenic Mouse Core. We thank Ran Brosh and Andrew Holland for plasmid construction reagents. This work was funded by National Institute of General Medical Sciences (NIGMS, USA) grant to P.W.J. (R01GM11755), Office of Research Infrastructure Programs (ORIP, USA) grant to P.W.J. (R21OD023720), Johns Hopkins University (JHU, USA) Discovery grant to P.W.J, and training grant fellowship from the National Cancer Institute (NCI, USA) to M.J.X. (T32CA009110).

References

Aragón L, 2018 The Smc5/6 complex: new and old functions of the enigmatic longdistance relative. Annu. Rev. Genet 52, 89–107. 10.1146/annurev-genet-120417-031353. [PubMed: 30476445]

Avior Y, Sagi I, Benvenisty N, 2016 Pluripotent stem cells in disease modelling and drug discovery. Nat. Rev. Mol. Cell Biol 17, 170–182. 10.1038/nrm.2015.27. [PubMed: 26818440]

Baker O, Gupta A, Obst M, Zhang Y, Anastassiadis K, Fu J, Stewart AF, 2016 RAC-tagging: recombineering And Cas9-assisted targeting for protein tagging and conditional analyses. Sci. Rep 6, 25529 10.1038/srep25529. [PubMed: 27216209]

Bence M, Jankovics F, Lukácsovich T, Erdélyi M, 2017 Combining the auxin- inducible degradation system with CRISPR/Cas9-based genome editing for the conditional depletion of endogenous Drosophila melanogaster proteins. FEBS J. 284, 1056–1069. 10.1111/febs.14042. [PubMed: 28207183]

Borsos M, Perricone SM, Schauer T, Pontabry J, de Luca KL, de Vries SS, Ruiz- Morales ER, Torres-Padilla M-E, Kind J, 2019 Genome-lamina interactions are established de novo in the early mouse embryo. Nature 569, 729–733. 10.1038/s41586-019-1233-0. [PubMed: 31118510]

Brosh R, Hrynyk I, Shen J, Waghray A, Zheng N, Lemischka IR, 2016 A dual molecular analogue tuner for dissecting protein function in mammalian cells. Nat. Commun 7, 11742 10.1038/ncomms11742. [PubMed: 27230261]

Camlin NJ, Evans JP, 2019 Auxin-inducible protein degradation as a novel approach for protein depletion and reverse genetic discoveries in mammalian oocytes†. Biol. Reprod 101, 704–718. 10.1093/biolre/ioz113. [PubMed: 31299080]

Casola S, 2010 Mouse models for miRNA expression: the ROSA26 locus. Methods Mol. Biol 667, 145–163. 10.1007/978-1-60761-811-9_10. [PubMed: 20827532]

Chen S, Lee B, Lee A-Y-F, Modzelewski AJ, He L, 2016 Highly efficient mouse genome editing by CRISPR ribonucleoprotein electroporation of zygotes. J. Biol. Chem 291, 14457–14467. 10.1074/jbc.M116.733154. [PubMed: 27151215]

Chen Y, Cao J, Xiong M, Petersen AJ, Dong Y, Tao Y, Huang C-T-L, Du Z, Zhang S-C, 2015 Engineering human stem cell lines with inducible gene knockout using CRISPR/Cas9. Cell Stem Cell 17, 233–244. 10.1016/j.stem.2015.06.001. [PubMed: 26145478]

Chen-Tsai RY, 2020 Integrase-mediated targeted transgenics through pronuclear microinjection. Methods Mol. Biol 2066, 35–46. 10.1007/978-1-4939-9837-1_3. [PubMed: 31512205]

Clift D, McEwan WA, Labzin LI, Konieczny V, Mogessie B, James LC, Schuh M, 2017 A method for the acute and rapid degradation of endogenous proteins. Cell 171, 1692–1706.e18. 10.1016/j.cell.2017.10.033.

Croft CL, Futch HS, Moore BD, Golde TE, 2019 Organotypic brain slice cultures to model neurodegenerative proteinopathies. Mol. Neurodegener 14, 45 10.1186/s13024-019-0346-0 [PubMed: 31791377]

Di Domenico AI, Christodoulou I, Pells SC, McWhir J, Thomson AJ, 2008 Sequential genetic modification of the hprt locus in human ESCs combining gene targeting and recombinase-mediated cassette exchange. Cloning Stem Cells 10, 217–230. 10.1089/clo.2008.0016. [PubMed: 18386992]

El-Brolosy MA, Stainier DYR, 2017 Genetic compensation: a phenomenon in search of mechanisms. PLoS Genet. 13, e1006780 10.1371/journal.pgen.1006780.

Ericsson AC, Crim MJ, Franklin CL, 2013 A brief history of animal modeling. Mo Med 110, 201–205. [PubMed: 23829102]

Fazzio TG, Panning B, 2010 Condensin complexes regulate mitotic progression and interphase chromatin structure in embryonic stem cells. J. Cell Biol 188, 491–503. 10.1083/jcb.200908026. [PubMed: 20176923]

Fisher CL, Marks H, Cho L-T-Y, Andrews R, Wormald S, Carroll T, Iyer V, Tate P, Rosen B, Stunnenberg HG, Fisher AG, Skarnes WC, 2017 An efficient method for generation of bi-allelic null mutant mouse embryonic stem cells and its application for investigating epigenetic modifiers. Nucl. Acids Res 45, e174 10.1093/nar/gkx811.

Friman ET, Deluz C, Meireles-Filho AC, Govindan S, Gardeux V, Deplancke B, Suter DM, 2019 Dynamic regulation of chromatin accessibility by pluripotency transcription factors across the cell cycle. eLife 8 10.7554/eLife.50087.

Gabdoulline R, Kaisers W, Gaspar A, Meganathan K, Doss MX, Jagtap S, Hescheler J, Sachinidis A, Schwender H, 2015 Differences in the early development of human and mouse embryonic stem cells. PLoS One 10, e0140803. 10.1371/journal.pone.0140803.

Gaddipati H, Pryzhkova MV, Jordan PW, 2019 Conditional mutation of SMC5 in mouse embryonic fibroblasts. Methods Mol. Biol 2004, 35–46. 10.1007/978-1-4939-9520-2_4. [PubMed: 31147908]

Gallego-Paez LM, Tanaka H, Bando M, Takahashi M, Nozaki N, Nakato R, Shirahige K, Hirota T, 2014 Smc5/6-mediated regulation of replication progression contributes to chromosome assembly during mitosis in human cells. Mol. Biol. Cell 25, 302–317. 10.1091/mbc.E13-01-0020. [PubMed: 24258023]

Gerlai R, 2016 Gene targeting using homologous recombination in embryonic stem cells: the future for behavior genetics? Front. Genet 7, 43 10.3389/fgene.2016.00043. [PubMed: 27148349]

Gu B, Posfai E, Rossant J, 2018 Efficient generation of targeted large insertions by microinjection into two-cell-stage mouse embryos. Nat. Biotechnol 36, 632–637. 10.1038/nbt.4166. [PubMed: 29889212]

Hippenmeyer S, Youn YH, Moon HM, Miyamichi K, Zong H, Wynshaw-Boris A, Luo L, 2010 Genetic mosaic dissection of Lis1 and Ndel1 in neuronal migration. Neuron 68, 695–709. 10.1016/j.neuron.2010.09.027. [PubMed: 21092859]

Holland AJ, Fachinetti D, Han JS, Cleveland DW, 2012 Inducible, reversible system for the rapid and complete degradation of proteins in mammalian cells. Proc. Natl. Acad. Sci. U.S.A 109, E3350–7. 10.1073/pnas.1216880109. [PubMed: 23150568]

Housden BE, Muhar M, Gemberling M, Gersbach CA, Stainier DYR, Seydoux G, Mohr SE, Zuber J, Perrimon N, 2017 Loss-of-function genetic tools for animal models: cross-species and cross-platform differences. Nat. Rev. Genet 18, 24–40. 10.1038/nrg.2016.118. [PubMed: 27795562]

Hsu PD, Scott DA, Weinstein JA, Ran FA, Konermann S, Agarwala V, Li Y, Fine EJ, Wu X, Shalem O, Cradick TJ, Marraffini LA, Bao G, Zhang F, 2013 DNA targeting specificity of RNA-guided Cas9 nucleases. Nat. Biotechnol 31, 827–832. 10.1038/nbt.2647. [PubMed: 23873081]

Hwang G, Sun F, O'Brien M, Eppig JJ, Handel MA, Jordan PW, 2017 SMC5/6 is required for the formation of segregation-competent bivalent chromosomes during meiosis I in mouse oocytes. Development 144, 1648–1660. 10.1242/dev.145607. [PubMed: 28302748]

Irion S, Luche H, Gadue P, Fehling HJ, Kennedy M, Keller G, 2007 Identification and targeting of the ROSA26 locus in human embryonic stem cells. Nat. Biotechnol 25, 1477–1482. 10.1038/nbt1362. [PubMed: 18037879]

John JA, Blogg CD, Murray FJ, Schwetz BA, Gehring PJ, 1979 Teratogenic effects of the plant hormone indole-3-acetic acid in mice and rats. Teratology 19, 321–324. 10.1002/tera.1420190307. [PubMed: 473083]

Kim H, Kim M, Im S-K, Fang S, 2018 Mouse Cre-LoxP system: general principles to determine tissue-specific roles of target genes. Lab. Anim. Res 34, 147–159. 10.5625/lar.2018.34.4.147. [PubMed: 30671100]

Lambrus BG, Moyer TC, Holland AJ, 2018 Applying the auxin-inducible degradation system for rapid protein depletion in mammalian cells. Methods Cell Biol. 144, 107–135. 10.1016/bs.mcb.2018.03.004. [PubMed: 29804665]

Lambrus BG, Uetake Y, Clutario KM, Daggubati V, Snyder M, Sluder G, Holland AJ, 2015 p53 protects against genome instability following centriole duplication failure. J. Cell Biol 210, 63–77. 10.1083/jcb.201502089. [PubMed: 26150389]

Lancaster MA, Huch M, 2019 Disease modelling in human organoids. Dis. Model. Mech 12 10.1242/dmm.039347.

Li M, Yu JSL, Tilgner K, Ong SH, Koike-Yusa H, Yusa K, 2018 Genome-wide CRISPR-KO screen uncovers mTORC1-mediated Gsk3 regulation in naive pluripotency maintenance and dissolution. Cell Rep. 24, 489–502. 10.1016/j.celrep.2018.06.027. [PubMed: 29996108]

Li S, Prasanna X, Salo VT, Vattulainen I, Ikonen E, 2019 An efficient auxin-inducible degron system with low basal degradation in human cells. Nat. Methods 16, 866–869. 10.1038/s41592-019-0512-x. [PubMed: 31451765]

Lyndaker AM, Lim PX, Mleczko JM, Diggins CE, Holloway JK, Holmes RJ, Kan R, Schlafer DH, Freire R, Cohen PE, Weiss RS, 2013 Conditional inactivation of the DNA damage response gene Hus1 in mouse testis reveals separable roles for components of the RAD9-RAD1-HUS1 complex in meiotic chromosome maintenance. PLoS Genet. 9, e1003320 10.1371/journal.pgen.1003320.

Miura K, Matoba S, Ogonuki N, Namiki T, Ito J, Kashiwazaki N, Ogura A, 2018 Application of auxin-inducible degron technology to mouse oocyte activation with PLCζ. J. Reprod. Dev 64, 319–326. 10.1262/jrd.2018-053. [PubMed: 29731504]

Morawska M, Ulrich HD, 2013 An expanded tool kit for the auxin-inducible degron system in budding yeast. Yeast 30, 341–351. 10.1002/yea.2967. [PubMed: 23836714]

Mourão LRMB, Santana RSS, Paulo LM, Pugine SMP, Chaible LM, Fukumasu H, Dagli MLZ, de Melo MP, 2009 Protective action of indole-3- acetic acid on induced hepatocarcinoma in mice. Cell Biochem. Funct 27, 16–22. 10.1002/cbf.1528. [PubMed: 19107877]

Nagy A, Gertsenstein M, Vintersten K, Behringer R, 2003 Manipulating the Mouse Embryo: A Laboratory Manual, third ed. Cold Spring Harbor Laboratory Press, Cold Spring Harbor (New York).

Natsume T, Kanemaki MT, 2017 Conditional degrons for controlling protein expression at the protein level. Annu. Rev. Genet 51, 83–102. 10.1146/annurev-genet-120116-024656. [PubMed: 29178817]

Natsume T, Kiyomitsu T, Saga Y, Kanemaki MT, 2016 Rapid protein depletion in human cells by auxin-inducible degron tagging with short homology donors. Cell Rep. 15, 210–218. 10.1016/j.celrep.2016.03.001. [PubMed: 27052166]

Nishide K, Hirano T, 2014 Overlapping and non-overlapping functions of condensins I and II in neural stem cell divisions. PLoS Genet. 10, e1004847 10.1371/journal.pgen.1004847.

Nishimura K, Fukagawa T, Takisawa H, Kakimoto T, Kanemaki M, 2009 An auxin- based degron system for the rapid depletion of proteins in nonplant cells. Nat. Methods 6, 917–922. 10.1038/nmeth.1401. [PubMed: 19915560]

Nora EP, Goloborodko A, Valton A-L, Gibcus JH, Uebersohn A, Abdennur N, Dekker J, Mirny LA, Bruneau BG, 2017 Targeted degradation of CTCF decouples local insulation of chromosome domains from genomic compartmentalization. Cell 169, 930–944.e22. 10.1016/j.cell.2017.05.004.

Oji A, Noda T, Fujihara Y, Miyata H, Kim YJ, Muto M, Nozawa K, Matsumura T, Isotani A, Ikawa M, 2016 CRISPR/Cas9 mediated genome editing in ES cells and its application for chimeric analysis in mice. Sci. Rep 6, 31666 10.1038/srep31666. [PubMed: 27530713]

Owens N, Papadopoulou T, Festuccia N, Tachtsidi A, Gonzalez I, Dubois A, Vandormael-Pournin S, Nora EP, Bruneau BG, Cohen-Tannoudji M, Navarro P, 2019 CTCF confers local nucleosome resiliency after DNA replication and during mitosis. eLife 8 10.7554/eLife.47898.

Paix A, Folkmann A, Goldman DH, Kulaga H, Grzelak MJ, Rasoloson D, Paidemarry S, Green R, Reed RR, Seydoux G, 2017 Precision genome editing using synthesis-dependent repair of Cas9-induced DNA breaks. Proc. Natl. Acad. Sci. U.S.A 114, E10745–E10754. 10.1073/pnas.1711979114.

Perez-Arnaiz P, Bruck I, Kaplan DL, 2016 Mcm10 coordinates the timely assembly and activation of the replication fork helicase. Nucl. Acids Res 44, 315–329. 10.1093/nar/gkv1260. [PubMed: 26582917]

Pryzhkova MV, Jordan PW, 2016 Conditional mutation of Smc5 in mouse embryonic stem cells perturbs condensin localization and mitotic progression. J. Cell Sci 129, 1619–1634. 10.1242/jcs.179036. [PubMed: 26919979]

Pryzhkova MV, Jordan PW, 2020 Adaptation of human testicular niche cells for pluripotent stem cell and testis development research. Tissue Eng. Regen. Med 17, 223–235. 10.1007/s13770-020-00240-0. [PubMed: 32114677]

Qin W, Dion SL, Kutny PM, Zhang Y, Cheng AW, Jillette NL, Malhotra A, Geurts AM, Chen Y-G, Wang H, 2015 Efficient CRISPR/Cas9-mediated genome editing in mice by zygote electroporation of nuclease. Genetics 200, 423–430. 10.1534/genetics.115.176594. [PubMed: 25819794]

Sakurai K, Shimoji M, Tahimic CGT, Aiba K, Kawase E, Hasegawa K, Amagai Y, Suemori H, Nakatsuji N, 2010 Efficient integration of transgenes into a defined locus in human embryonic stem cells. Nucl. Acids Res 38, e96 10.1093/nar/gkp1234.

Sathyan KM, McKenna BD, Anderson WD, Duarte FM, Core L, Guertin MJ, 2019 An improved auxin-inducible degron system preserves native protein levels and enables rapid and specific protein depletion. Genes Dev. 33, 1441–1455. 10.1101/gad.328237.119. [PubMed: 31467088]

Sato T, Katagiri K, Kojima K, Komeya M, Yao M, Ogawa T, 2015 In vitro spermatogenesis in explanted adult mouse testis tissues. PLoS One 10, e0130171. 10.1371/journal.pone.0130171.

Shamir ER, Ewald AJ, 2014 Three-dimensional organotypic culture: experimental models of mammalian biology and disease. Nat. Rev. Mol. Cell Biol 15, 647–664. 10.1038/nrm3873. [PubMed: 25237826]

Slaymaker IM, Gao L, Zetsche B, Scott DA, Yan WX, Zhang F, 2016 Rationally engineered Cas9 nucleases with improved specificity. Science 351, 84–88. 10.1126/science.aad5227. [PubMed: 26628643]

Smith JR, Maguire S, Davis LA, Alexander M, Yang F, Chandran S, ffrench-Constant C, Pedersen RA, 2008 Robust, persistent transgene expression in human embryonic stem cells is achieved with AAVS1-targeted integration. Stem Cells 26, 496–504. 10.1634/stemcells.2007-0039. [PubMed: 18024421]

Staal FJT, Pike-Overzet K, Ng YY, van Dongen JJM, 2008 Sola dosis facit venenum. Leukemia in gene therapy trials: a question of vectors, inserts and dosage? Leukemia 22, 1849–1852. 10.1038/leu.2008.219. [PubMed: 18769449]

Stephan AK, Kliszczak M, Dodson H, Cooley C, Morrison CG, 2011 Roles of vertebrate Smc5 in sister chromatid cohesion and homologous recombinational repair. Mol. Cell. Biol 31, 1369–1381. 10.1128/MCB.00786-10. [PubMed: 21245390]

Strathdee D, Ibbotson H, Grant SGN, 2006 Expression of transgenes targeted to the Gt(ROSA)26Sor locus is orientation dependent. PLoS One 1, e4. 10.1371/journal.pone.0000004.

Sybirna A, Tang WWC, Pierson Smela M, Dietmann S, Gruhn WH, Brosh R, Surani MA, 2020 A critical role of PRDM14 in human primordial germ cell fate revealed by inducible degrons. Nat. Commun 11, 1282 10.1038/s41467-020-15042-0. [PubMed: 32152282]

Tam PPL, Rossant J, 2003 Mouse embryonic chimeras: tools for studying mammalian development. Development 130, 6155–6163. 10.1242/dev.00893. [PubMed: 14623817]

Tasic B, Hippenmeyer S, Wang C, Gamboa M, Zong H, Chen-Tsai Y, Luo L, 2011 Site-specific integrase-mediated transgenesis in mice via pronuclear injection. Proc. Natl. Acad. Sci. U.S.A 108, 7902–7907. 10.1073/pnas.1019507108. [PubMed: 21464299]

Tröder SE, Ebert LK, Butt L, Assenmacher S, Schermer B, Zevnik B, 2018 An optimized electroporation approach for efficient CRISPR/Cas9 genome editing in murine zygotes. PLoS One 13, e0196891. 10.1371/journal.pone.0196891.

Trost M, Blattner AC, Lehner CF, 2016 Regulated protein depletion by the auxin- inducible degradation system in Drosophila melanogaster. Fly (Austin) 10, 35–46. 10.1080/19336934.2016.1168552. [PubMed: 27010248]

Wang W, Kutny PM, Byers SL, Longstaff CJ, DaCosta MJ, Pang C, Zhang Y, Taft RA, Buaas FW, Wang H, 2016 Delivery of Cas9 protein into mouse zygotes through a series of electroporation dramatically increases the efficiency of model creation. J. Genet. Genomics 43, 319–327. 10.1016/j.jgg.2016.02.004. [PubMed: 27210041]

Wood L, Booth DG, Vargiu G, Ohta S, deLima Alves F, Samejima K, Fukagawa T, Rappsilber J, Earnshaw WC, 2016 Auxin/AID versus conventional knockouts: distinguishing the roles of CENP-T/W in mitotic kinetochore assembly and stability. Open Biol. 6, 150230 10.1098/rsob.150230.

Wu N, Kong X, Ji Z, Zeng W, Potts PR, Yokomori K, Yu H, 2012 Scc1 sumoylation by Mms21 promotes sister chromatid recombination through counteracting Wapl. Genes Dev. 26, 1473–1485. 10.1101/gad.193615.112. [PubMed: 22751501]

Wutz G, Várnai C, Nagasaka K, Cisneros DA, Stocsits RR, Tang W, Schoenfelder S, Jessberger G, Muhar M, Hossain MJ, Walther N, Koch B, Kueblbeck M, Ellenberg J, Zuber J, Fraser P, Peters J-M, 2017 Topologically associating domains and chromatin loops depend on cohesin and are regulated by CTCF, WAPL, and PDS5 proteins. EMBO J. 36, 3573–3599. 10.15252/embj.201798004. [PubMed: 29217591]

Yesbolatova A, et al., 2019 Generation of conditional auxin-inducible degron (AID) cells and tight control of degron-fused proteins using the degradation inhibitor auxinole. Methods 164–165, 73–80. 10.1016/j.ymeth.2019.04.010.

Zeng H, Horie K, Madisen L, Pavlova MN, Gragerova G, Rohde AD, Schimpf BA, Liang Y, Ojala E, Kramer F, Roth P, Slobodskaya O, Dolka I, Southon EA, Tessarollo L, Bornfeldt KE, Gragerov A, Pavlakis GN, Gaitanaris GA, 2008 An inducible and reversible mouse genetic rescue system. PLoS Genet. 4, e1000069 10.1371/journal.pgen.1000069.

Zhang L, Ward JD, Cheng Z, Dernburg AF, 2015 The auxin-inducible degradation (AID) system enables versatile conditional protein depletion in C. elegans. Development 142, 4374–4384. 10.1242/dev.129635. [PubMed: 26552885]

Zhu F, Gamboa M, Farruggio AP, Hippenmeyer S, Tasic B, Schüle B, Chen- Tsai Y, Calos MP, 2014 DICE, an efficient system for iterative genomic editing in human pluripotent stem cells. Nucl. Acids Res 42, e34 10.1093/nar/gkt1290.

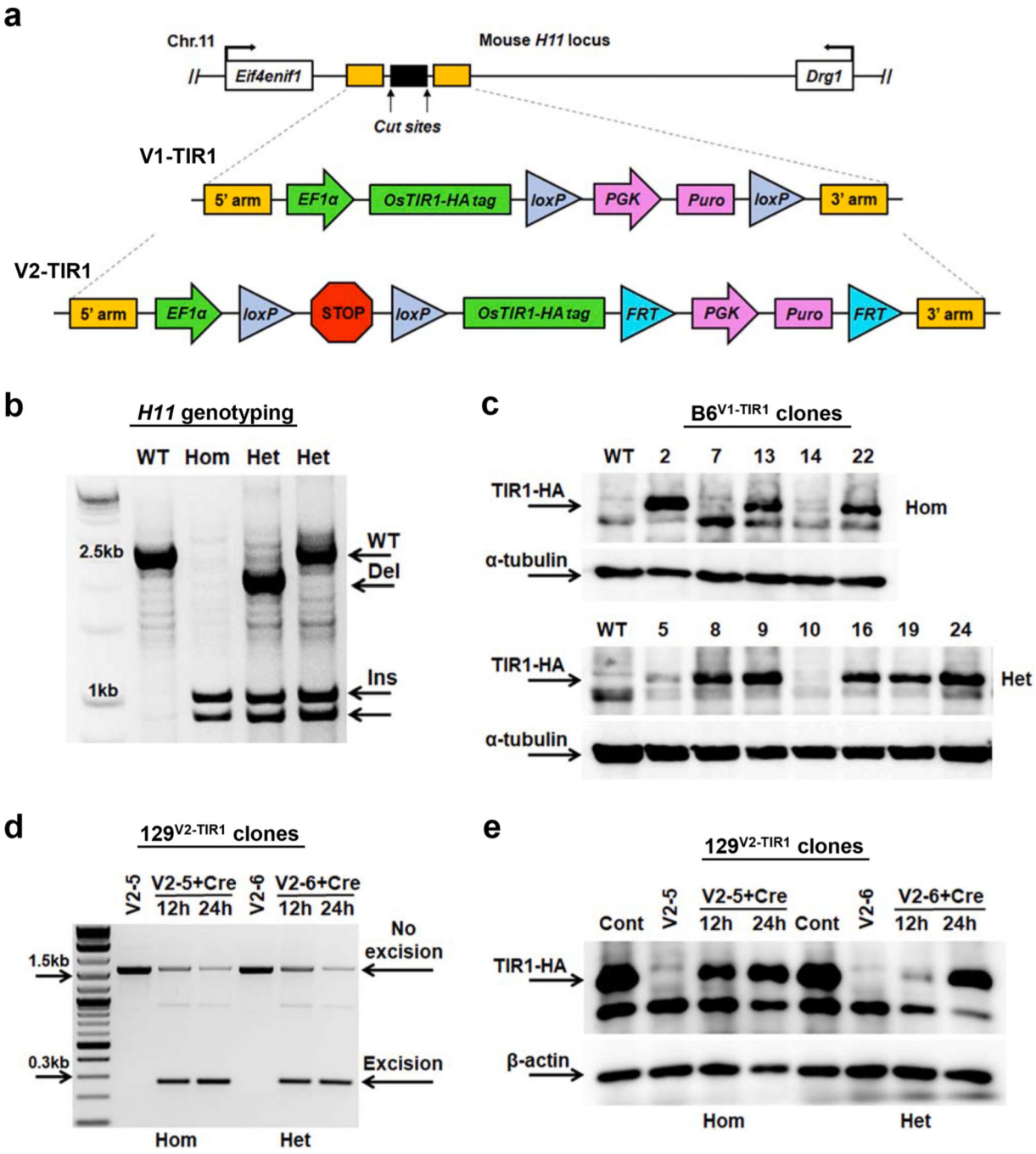

Fig. 1.

Integration of *TIR1* expression cassette into mouse *H11* locus and evaluation of protein expression. (a) Schematic representation of *H11* locus targeting strategy and DNA donor construct design. (b) An example of expected PCR products used for the identification of targeted homozygous (Hom) and heterozygous (Het) mESC clones. Arrows indicate 2782 bp wild type (WT), 1607 bp deletion (Del), and the two insertion (Ins) bands, 1027 bp (3′ arm) and 922 bp (5′ arm). (c) Western blot analysis of TIR1 expression in $B6^{V1\text{-}TIR1}$ homozygous (Hom) and heterozygous (Het) mESC clones using anti-HA tag antibodies, α-tubulin was

used as a loading control. Numbers above each lane represent the clone isolate number. (d) Genotyping of homozygous (Hom, V2–5) and heterozygous (Het, V2–6) $129^{V2\text{-}TIR1}$ mESC clones showing expected PCR products upon Cre-mediated STOP cassette excision 12 and 24 h post-transfection. Arrows show 1652 bp fragment indicative of *TIR1* transgene with present STOP cassette (No excision) and 269 bp fragment indicative of *TIR1* transgene with excised STOP cassette (Excision). (e) Western blot analysis of TIR1 expression in homozygous (Hom, V2–5) and heterozygous (Het, V2–6) $129^{V2\text{-}TIR1}$ mESCs 12 and 24 h post-transfection. β-actin served as a loading control. $B6^{V1\text{-}TIR1}$ mESCs were used as a control for TIR1 expression. Full-length blots are presented in Fig. S8.

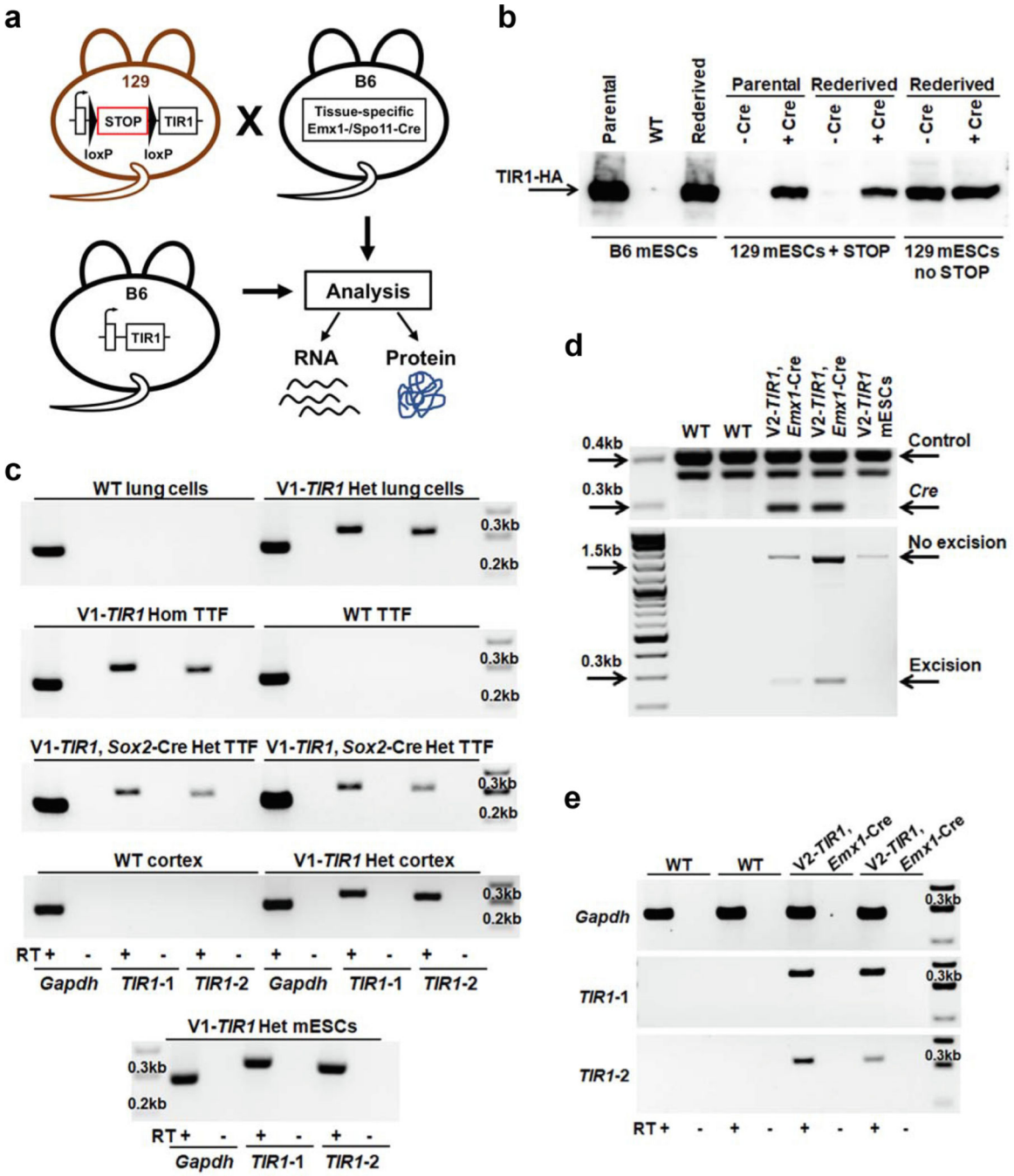

Fig. 2.

Evaluation of *TIR1* transgene expression in mice. (a) An outline of $B6^{V1\text{-}TIR1}$ and $129^{V2\text{-}TIR1}$ transgenic mice analysis. (b) Western blot analysis of TIR1 expression in mESCs derived from $B6^{V1\text{-}TIR1}$ and $129^{V2\text{-}TIR1}$ transgenic mice with or without the floxed STOP cassette, which was excised *in vivo*. (c) RT-PCR analysis of *TIR1* expression in different tissues from wild type (WT) and $B6^{V1\text{-}TIR1}$ transgenic mice: primary cultures of lung cells, tail tip fibroblasts (TTF) and cortex tissue. Mice were analyzed at postnatal day 2 through day 10. Two pairs of primers (*TIR1*-1 and *TIR1*-2) were used to detect RNA expression of

TIR1. *Gapdh* was used as an internal control. Reverse transcriptase-negative reactions are provided for each sample. $B6^{V1\text{-}TIR1}$ mESCs were used as a positive control for *TIR1* expression (d) PCR genotyping of 12.5 dpc wild type (WT) and $129^{V2\text{-}TIR1}$ embryonic cortices showing *in vivo* excision of the floxed STOP cassette, mediated by *Emx1-Cre*. Two WT and two $129^{V2\text{-}TIR1}$ mice from breeding with *Emx1-Cre* mice were used for analysis. Arrows show 420 bp internal PCR control (*Cpxm*) band (Control), 281 bp *Cre* transgene (*Cre*), 1652 bp fragment of *TIR1* transgene with STOP cassette (No excision) and 269 bp fragment of *TIR1* transgene with excised STOP cassette (Excision). (e) RT-PCR analysis of *TIR1* expression in 12.5dpc wild type (WT) and $129^{V2\text{-}TIR1}$ embryonic cortices from (d). Full-length blot and gels are presented in Fig. S10.

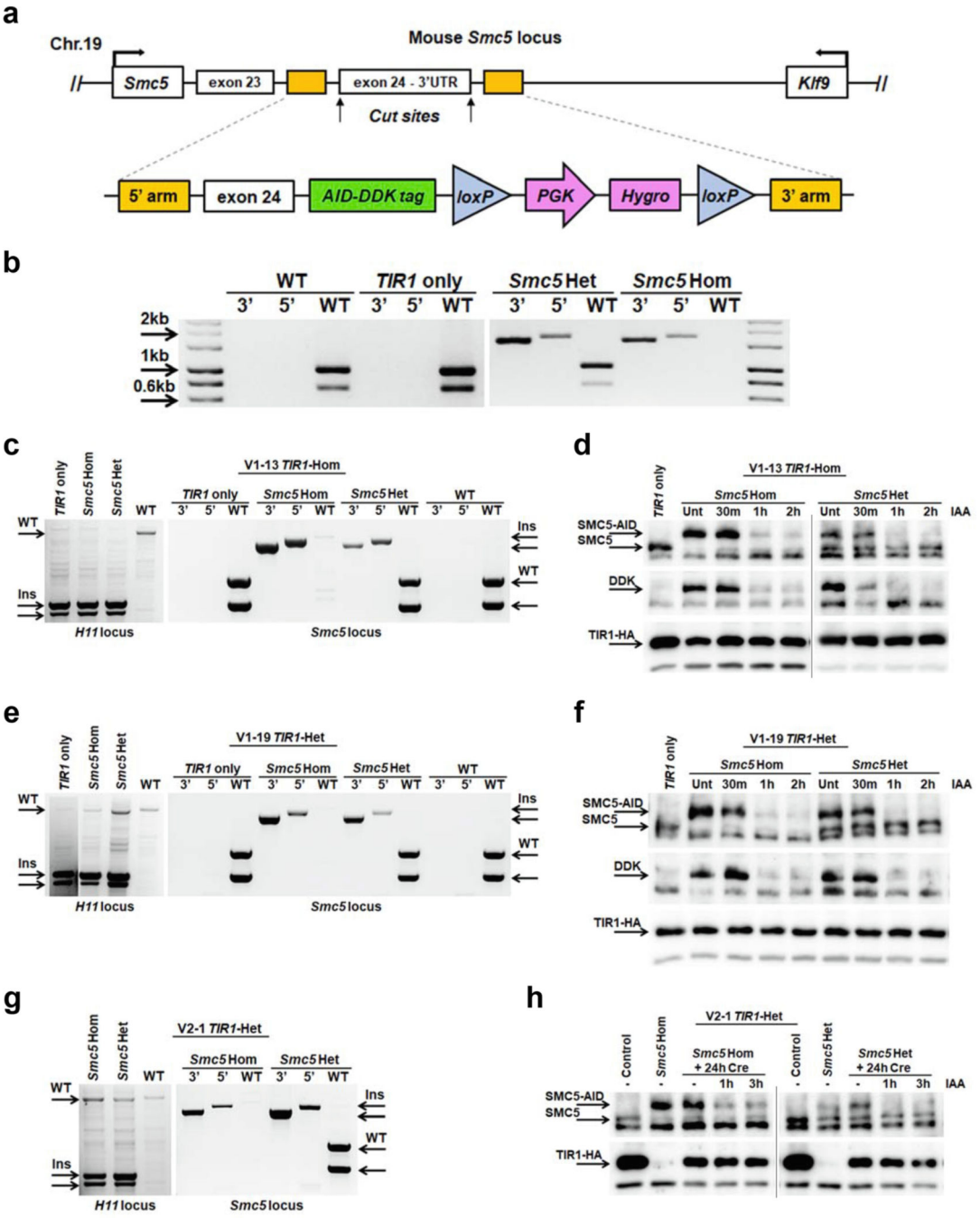

Fig. 3.

Smc5 locus targeting and evaluation of auxin-mediated protein degradation. (a) Schematic representation of *Smc5* locus targeting strategy and DNA donor construct design. (b) An example of expected PCR products used for the identification of targeted homozygous (*Smc5* Hom) and heterozygous (*Smc5* Het) mESC clones: 746 bp and 1020 bp wild type (WT) fragments, 1641 bp - integration at 3′arm site (3′) and 1775 bp - integration at 5′ arm site (5′). (c) PCR genotyping of *H11* and *Smc5* locus of wild type (WT), parental B6$^{V1\text{-}TIR1}$ V1–13 *TIR1* homozygous (*TIR1* only) and its derivatives *Smc5-AID* homozygous (*Smc5*

Hom) and heterozygous (*Smc5* Het) mESC lines. Arrows indicate the presence or absence of characteristic wild type (WT) and transgene insertion (Ins) bands. (d) Western blot analysis of auxin (IAA)-induced SMC5-AID protein depletion at 30 min, 1 h, and 2 h of treatment in $B6^{V1\text{-}TIR1}$ mESCs from (c). SMC5-AID protein levels were assessed using anti- SMC5 and anti-DDK antibodies. Unt – cells not treated with auxin. (e) PCR genotyping of *H11* and *Smc5* locus of wild type (WT), parental $B6^{V1\text{-}TIR1}$ V1–19 *TIR1* heterozygous (*TIR1* only) and its derivatives *Smc5-AID* homozygous (*Smc5* Hom) and heterozygous (*Smc5* Het) mESC lines. Arrows indicate the presence or absence of characteristic wild type (WT) and transgene insertion (Ins) bands. Genotyping results of *H11* locus for "*TIR1* only" sample was enhanced to show the presence of the WT band. (f) Western blot analysis of auxin (IAA)-induced SMC5-AID protein depletion at 30 min, 1 h, and 2 h of treatment in $B6^{V1\text{-}TIR1}$ mESCs from (e). SMC5-AID protein levels were assessed using anti-SMC5 and anti-DDK antibodies. Unt – cells not treated with auxin. (g) PCR genotyping of *H11* and *Smc5* locus of *Smc5-AID* homozygous (*Smc5* Hom) and heterozygous (*Smc5* Het) mESC lines derived from parental $129^{V2\text{-}TIR1}$ V2–1 *TIR1* heterozygous mESC line. Arrows indicate the presence or absence of characteristic wild type (WT) and transgene insertion (Ins) bands. (h) Western blot analysis of SMC5-AID protein depletion in $129^{V2\text{-}TIR1}$ mESCs from (g). At 24 h post-transfection with *Cre* recombinase cells were treated with auxin (IAA) for 1 h and 3 h. SMC5-AID protein levels were assessed using anti-SMC5 antibodies, TIR1 upregulation was detected using anti-HA tag antibodies. $B6^{V1\text{-}TIR1}$ mESCs were used as a control for wild type SMC5 and TIR1 expression. Full- length blots are presented in Fig. S11.

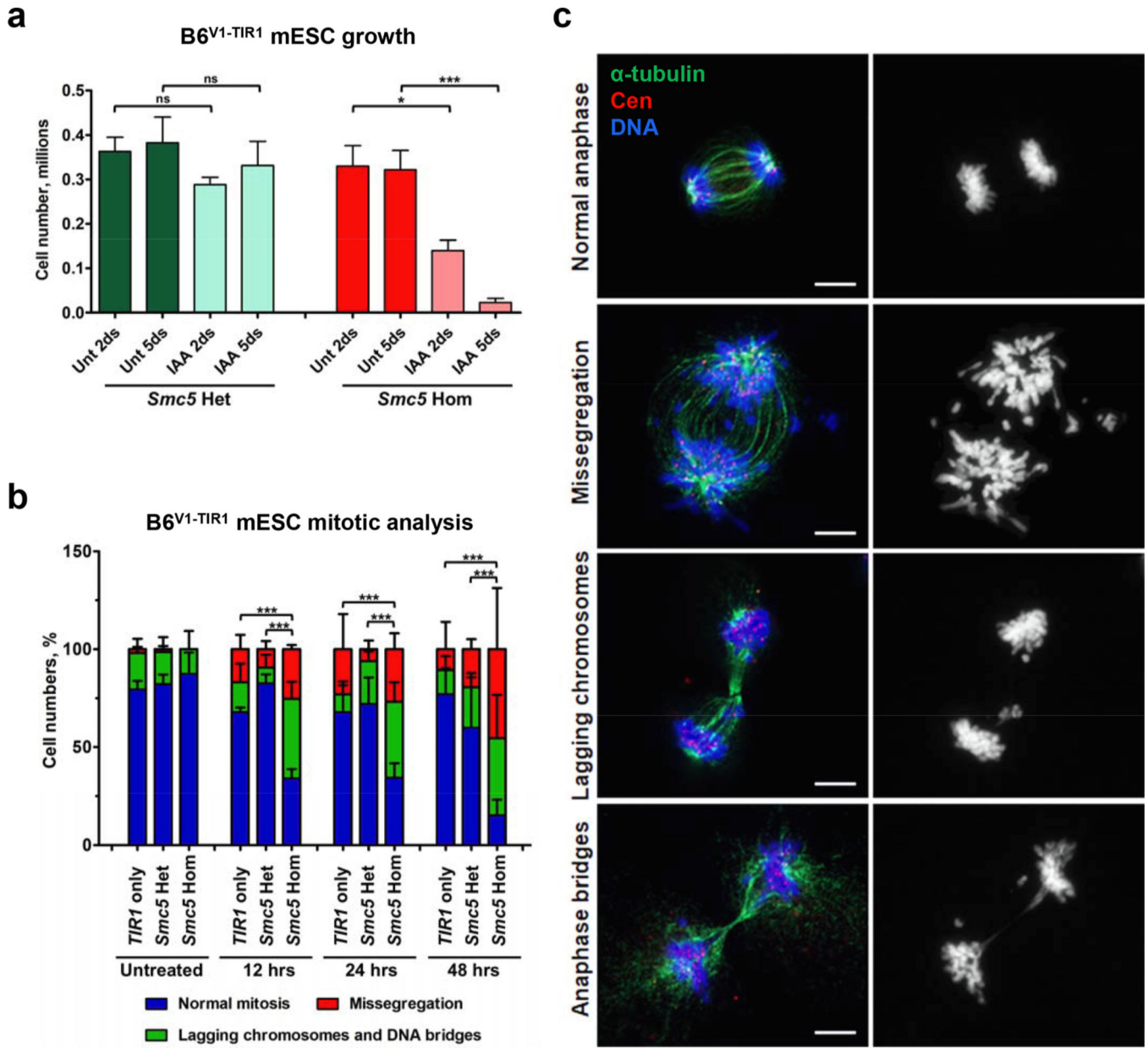

Fig. 4.

Evaluation of SMC5 depletion phenotype in mESCs. (a) Quantification of cell growth in SMC5-depleted and control B6$^{V1\text{-}TIR1}$ mESCs at two and five days of auxin (IAA) treatment. Unt – cells not treated with auxin. *Smc5* Het and *Smc5* Hom – *Smc5-AID* heterozygous and homozygous mESCs, respectively. Data are shown as the mean ± SEM (n = 4). Asterisks (*) indicate significant differences between groups (*p = 0.0104, ***p = 0.0005, ns – not significant, unpaired two-tailed Student's *t* test). (b) Twelve to sixteen hours after passaging parental B6$^{V1\text{-}TIR1}$ mESCs (*TIR1* only) and its derivatives *Smc5-AID* homozygous (*Smc5* Hom) and heterozygous (*Smc5* Het) mESCs were treated with auxin for 12, 24 and 48 h. Not treated with auxin cells (Untreated) were harvested at 48 h. The graph shows quantification of anaphase cells undergoing normal and abnormal mitosis. Data are

shown as the mean ± SD (n = 3). Asterisks (*) indicate significant differences between groups (***$p < 0.00047$, Pearson's chi-squared test with Yates' continuity correction). (c) Representative images of mitotic cells: normal anaphase, missegregation, lagging chromosomes and anaphase bridges. Scale bar represents 10 μm.

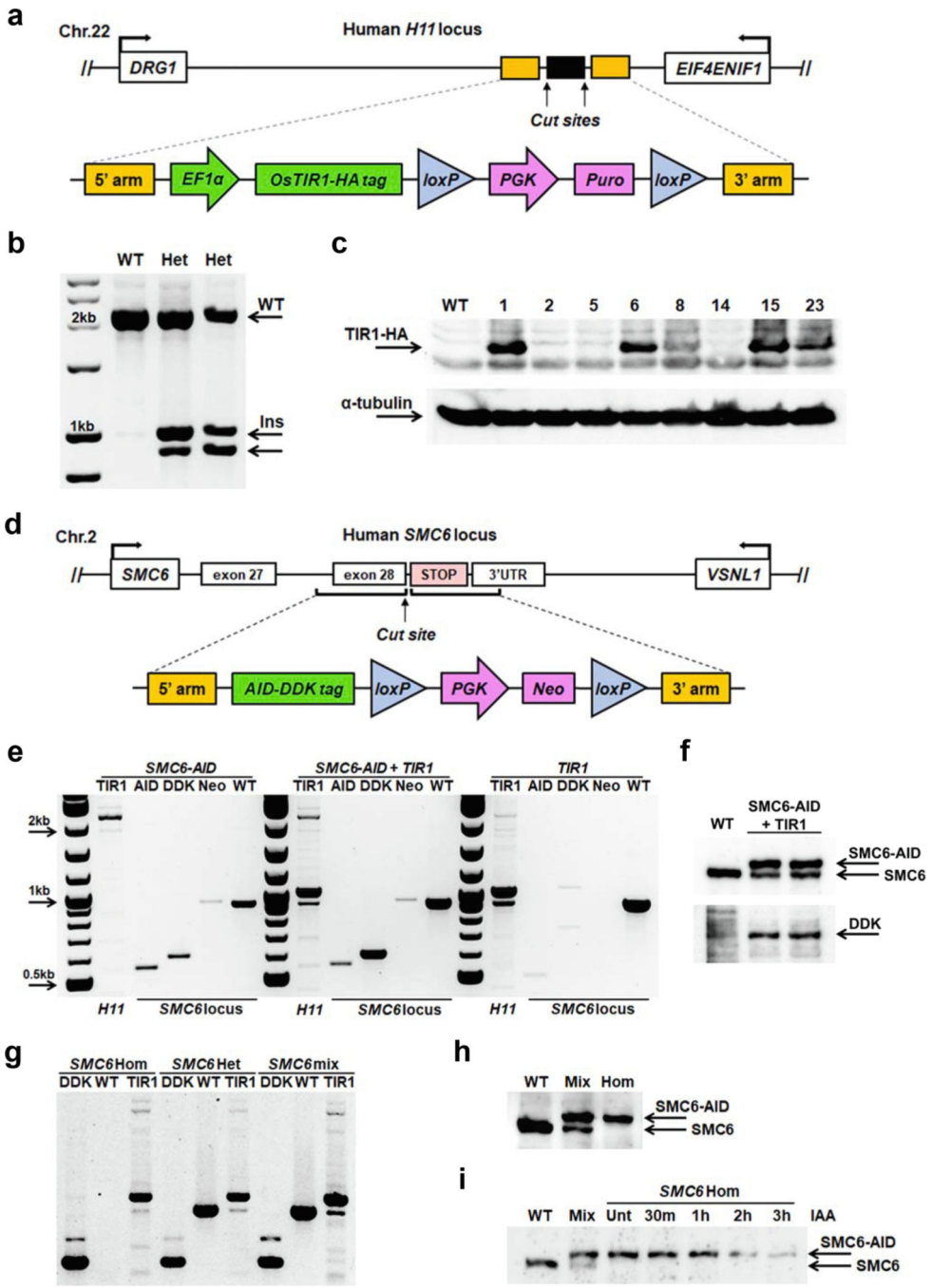

Fig. 5.

Integration of AID system into hESCs. (a) Schematic representation of *H11* locus targeting strategy and DNA donor construct design. (b) The example of expected PCR products used for the identification of *TIR1* transgenic hESCs. Arrows indicate 2204 bp wild type (WT) and 1017 bp (3′ arm) and 911 bp (5′ arm) insertion (Ins) bands. Het – heterozygote. (c) Western blot analysis of TIR1 expression in hESC clones using anti-HA tag antibodies, α-tubulin was used as a loading control. Numbers above the panel represent the clone isolate number. (d) Schematic representation of *SMC6* locus targeting strategy and DNA donor

construct design. (e) PCR genotyping of *SMC6-AID* and *TIR1* transgenic hESCs. *SMC6-AID* only and *TIR1* only transgenic hESCs served as controls. Expected PCR products for the identification of *SMC6-AID* transgenes are as follows: *AID*-tag 558 bp, *DDK* tag 605 bp, neomycin selection cassette (Neo) 927 bp and 923 bp wild type (WT). (f) Western blot analysis of AID- and DDK-tagged SMC6 expression in transgenic hESCs. SMC6-AID protein levels were assessed using anti-SMC6 and anti-DDK antibodies. (g) Example of expected PCR products used for identification of *SMC6-AID* and *-DDK*-tagged homozygous (Hom) and heterozygous (Het) transgenic hESCs. Not subcloned *SMC6-AID* + *TIR1* cells (mix) were used as a control. Band sizes are described in (b) and (e). (h) Western blot analysis showing characteristic bands for wild type, heterozygote and homozygote SMC6-AID cell lines, respectively. SMC6 protein levels were assessed using anti-SMC6 antibodies. (i) Western blot analysis showing the depletion of AID-tagged SMC6 protein in homozygous cell line upon auxin addition. Full-length blots are presented in Fig. S12.

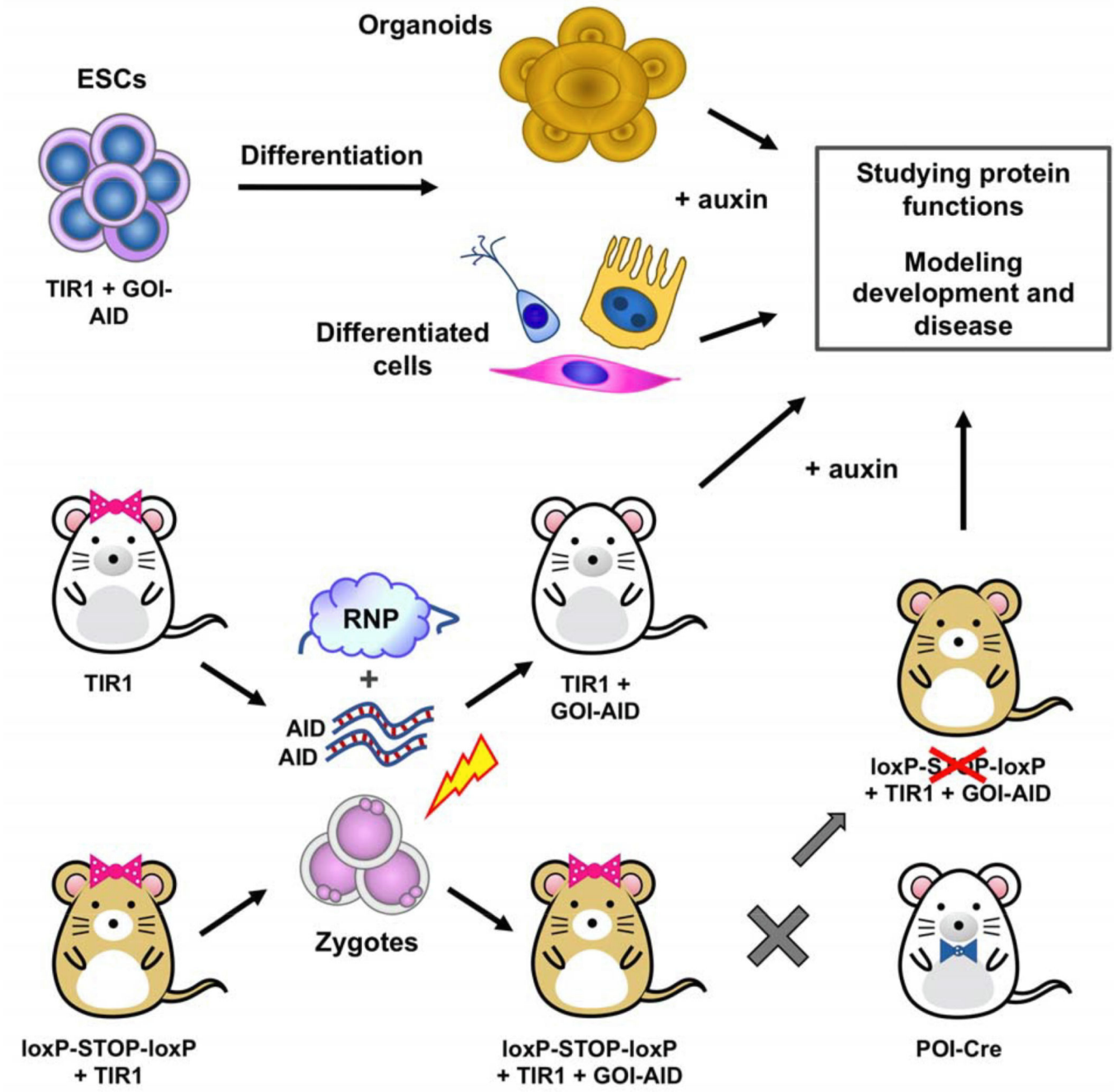

Fig. 6.

Summary of proposed applications of AID technology in stem cell research and transgenic mice. hESCs with integrated AID system can be differentiated directly into tissue-specific cell types or in 3D organoid culture and used for multiple applications, such as studying gene and protein functions, disease modeling and developmental studies. Mice with integrated AID system offer an opportunity to study protein functions *in vivo* and model diseased phenotypes at an organism or organ level. AID tagging of mouse endogenous genes can be efficiently performed by co-electroporating CRISPR-Cas9 system components and donor DNA oligos into zygotes. Constitutive or conditional (Cre-mediated) *TIR1* expression

can be employed to perform the research in a tissue or cell type-specific manner. RNP – ribonucleoprotein consisting of the Cas9 protein in complex with a targeting gRNA, GOI-AID – gene of interest tagged with AID, POI-Cre – Cre recombinase expression driven by the promoter of interest.